Egyptian Journal of Aquatic Biology & Fisheries
Zoology Department, Faculty of Science,
Ain Shams University, Cairo, Egypt.
ISSN 1110 – 6131
Vol. 28(2): 273 – 298 (2024)
www.ejabf.journals.ekb.eg
https://doi.10.21608/EJABF.2024.347834

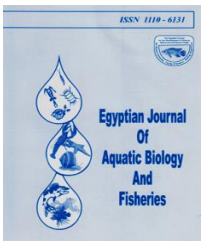

Hospital Wastewater Screening and Treatment Using Two Novel Magnetic Iron Nanocomposites

Amr B. Mostafa[1]*, Elham H.A. Ali[2], Ahmed M. Azzam[3], Michel F. Abdel-Messih[4], Mahmoud Abdelwahab Fathy[4], Sally M. Salaah[5], Magdy T. Khalil[1] , Marwa M. El-Naggar[1]

[1] Zoology Department, Faculty of Science, Ain Shams University, Egypt.
[2] Zoology Department, Faculty of Women for Arts, Science, and Education, Ain Shams University, Egypt.
[3] Environmental Research Department, Theodor Bilharz Research Institute (TBRI), Giza, 12411, Egypt.
[4] Chemistry Department, Faculty of Science, Ain Shams University, Egypt.
[5] National Institute of Oceanography and Fisheries, NIOF, Egypt.

*Corresponding Author: amrbayoumy@sci.asu.edu.eg

ARTICLE INFO
Article History:
Received: Feb. 29, 2024
Accepted: March 19, 2024
Online: March 30, 2024

Keywords:
Pharmaceutical,
Hospital,
Wastewater,
Fe_3O_4@SiO_2,
$NiFe_2O_4$,
Nanocomposites

ABSTRACT

Pharmaceutical pollutants in hospital wastewater (HWW) have the potential to contaminate both aquatic and terrestrial natural environments, posing a threat to aquatic life and human health. This work aimed to screen some chemical pollutants in HWW and evaluate the capacity of two magnetic nanocomposites (Fe_3O_4@SiO_2 and $NiFe_2O_4$ NCs) to remove these pollutants from HWW. The manufactured nanocomposites were described with different techniques. The collected HWW samples were screened by LCMS/ MS and HPLC/ UV before and after treatment to detect the capacity of certain pharmaceutical pollutants. The screening results of HWW showed that numerous different compounds belonging to diverse groups of drugs were found in the water samples. Both nanocomposites exhibited a significant activity in degradation, removing a high concentration of the pharmaceutical pollutants in treated HWW. Meanwhile, data based on HPLC/ UV analysis revealed that, $NiFe_2O_4$ NC was more effective than Fe_3O_4@SiO_2 NC, which removed more peaks of several selected compounds, indicating its capacity to reduce these pollutants. Therefore, the outcomes of the current research provided new innovative effective materials for treating hospital wastewater, which can contribute to preventing the spread of pollutants and preserving the aquatic environment.

INTRODUCTION

Wastewater emitted by human activity, from home, industrial, medical, and commercial sources, is referred to as sewage water. Organic debris, including nutrients (such as nitrogen and phosphate), pathogens (for example bacteria, viruses, and parasites), and a variety of chemicals are among the pollutants present in this water **(Kesari *et al.*, 2021)**. The River Nile provides a significant amount of water to millions of citizens in Egypt, where it is also used for agriculture. Unfortunately, there have been

worries about the River Nile being contaminated by a variety of wastewater sources including untreated hospital effluents. Hospital wastewater (HWW) contains a variety of new pollutants, viz. hormones, endocrine-disrupting substances, persistent organic pollutants (PCPs), and pharmaceutically active substances. These pollutants have the potential to permeate natural habitats, including aquatic and terrestrial ones, endangering both marine life and individual health.

Hospital effluent was proved to have significant quantities of several medications in a prior research **(Saguti *et al.*, 2021)**. However, municipal systems are not usually proposed to eliminate medical or pharmaceutical wastes. **Abdallah *et al.* (2020)** examined the existence of antibiotics and microorganisms resistant to antibiotics in effluent samples taken from three hospitals in Cairo, Egypt. High quantities of antibiotics and bacteria resistant to antibiotics were discovered in the studied hospital wastewater samples, suggesting the possibility of these toxins being released into the environment including the Nile River. To diminish the possible negative effects of hospital wastewater on the environment and public health, the need for better wastewater management and management procedures in hospitals was emphasized **(Yuan & Pia, 2023)**.

Utilizing nanotechnology to treat HWW has many benefits, one of which is that it may increase the efficiency of current treatment techniques. For instance, including nanoparticles in a biological treatment procedure might promote the elimination of pollutants and boost the effectiveness of the whole treatment process. Furthermore, compared to conventional approaches, treatment systems based on nanotechnology often operate at lower prices and with less energy usage. Some HWW treatment techniques based on nanotechnology include utilizing nanopores, which is a membrane-based filtration technique known as nanofiltration that removes pollutants from wastewater. Small molecules, including dissolved salts and organic debris, may be removed using nanofiltration. Via utilizing titanium dioxide and other photocatalytic nanoparticles, photocatalysis uses ultraviolet light to cleanse water and break down organic contaminants. Adsorption is the procedure of removing pollutants from the effluent by nanoparticles having a large surface area. Pathogens, organic contaminants, and heavy metals may all be eliminated upon applying this technique. The flow of nanoparticles into the environment has significant hazards, even though the application of nanotechnology in HWW treatment is promising. The possible hazards and advantages of employing nanotechnology in wastewater treatment are still being studied **(Zhang *et al.*, 2017; Zhang *et al.*, 2018; Khan *et al.*, 2019; Hamad & El-Sesy, 2023; Kumar *et al.*, 2023)**.

Research is still being done on the use of nanomaterials to remove hospital waste compounds from water. Nanoparticles investigated for this purpose include pharmaceuticals and heavy metals that would be removed from hospital wastewater using graphene oxide, which has been the subject of research in this area. It has been shown to have a high capacity for adsorption and to be readily removed from wastewater **(Wu *et al.*, 2019)**. Research suggested that silver nanoparticles possess antibacterial properties

and could potentially be effective in eradicating bacteria from hospital wastewater **(Li *et al.*, 2019)**. The removal of organic and heavy metal pollutants from hospital wastewater has been studied in relation to iron oxide nanoparticles. They can both absorb impurities and function as a catalytic agent for the oxidation of organic molecules **(Zhang *et al.*, 2018)**. Carbon-based nanoparticles showed that carbon-based nanoparticles, such as carbon nanotubes and graphene oxide, are efficient in removing pathogens, heavy metals, and organic pollutants from hospital wastewater **(Akhtar & Bhanger, 2010)**.

Magnetic nano-adsorbent materials have been used to treat wastewater in the present day. Recent study has focused on magnetic nano-adsorbent materials due to their capacity to eliminate organic pollutants from wastewater. Nano-magnetic adsorbents have some distinguishing qualities, including great surface area, extreme absorption capacity, and the ease of separation when using an external magnetic field. These properties reduce the likelihood to form a secondary pollutant. Magnetic nano-materials address the inadequacies of conservative adsorbents, which struggle to separate from contaminated solutions. Additionally, there have been few concerns regarding the modification of magnetic nano-adsorbents to enhance their capacity for removing specific organic contaminants **(Chen *et. al.*, 2019)**.

This study aimed to screen and identify the most frequently present chemical drugs in hospital wastewater (HWW) using Ain Shams Hospital HWW samples, Egypt, as a case study, given that it is one of Cairo's public hospitals. Furthermore, we synthesized and characterized two novel magnetic nanocomposites to evaluate their capacity for removing and treating these pharmaceutical pollutants in HWW, with the goal of establishing a safe treatment process.

MATERIALS AND METHODS

Materials

For the synthesis of all nanomaterials in this study, all chemicals were of an analytical grade and were thus used without further purification. Ferric chloride hexa-hydrate ($FeCl_3 \cdot 6H_2O$), ferrous chloride tetra-hydrate ($FeCl_2 \cdot 4H_2O$), (3-Aminopropyl) triethoxysilane (APTES), nickel chloride hexahydrate ($NiCl_2 \cdot 6H_2O$), and ammonium persulfate ($(NH_4)_2S_2O_8$) were purchased from Aldrich. Sodium hydroxide (NaOH) and hydrochloric acid (HCl) were obtained from Merck (Germany). Deionized water was used as a solvent to prepare each solution. The standards of chemicals of analgesics and antibiotics were purchased from Sigma.

Hospital wastewater (HWW) samples collection and screening

The hospital effluent (HWW) was monthly collected from the drainage lines of Ain Shams specialized hospital, with ten liters collected each time, over a period of six months. A small sample (50ml) was sent to the LCMS/ MS lab for screening allowing MWT. Another portion of the samples was analyzed using HPLC/ UV to identify the

concentration of analgesics and antibiotics (paracetamol, diclofenac, sulfamethoxazole, ketoprofen, amoxicillin, ofloxacin, and oxytetracycline). The most collected samples were spent in the different Nano treatment trials.

Synthesis of $NiFe_2O_4$ nanocomposite (NF NC)

Aqueous mixtures of ferric and nickel chloride were combined in a 1:2 molar ratio and continuously stirred for 30 minutes. An aqueous 2.0M NaOH solution was added to the mixture dropwise (1.0mL min^{-1}) until it reached a pH of 11. After stirring consistently for an hour, the mixture was heated to 100°C, producing a brown precipitate. To ensure stability, the mixture was let to stand overnight. The pH of the filtrate was adjusted to 7.0 by repeatedly washing the black precipitate with distilled water. The residue was collected and dried at 110°C for six hours. After being crushed into a fine powder, the material was calcined at 600°C for five hours before being kept in a desiccator **(Fathy *et al.*, 2022)**.

Preparation of $Fe_3O_4@SiO_2$ nanocomposite (FS NC)

Ferric chloride and ferrous chloride were mixed in a 2:1 molar ratio. The solutions of Fe^{2+} and Fe^{3+} were prepared by making their aqueous solutions in distilled water, and this solution containing both ions was then heated up to 50^{o}C for 10 min. After heating, the solution was precipitated by ammonia solution with a continuous stirring on the magnetic stirrer at 50^{o}C. Black colored particles of iron oxide Fe_3O_4 nanoparticles were precipitated. These particles were then separated from the solution using a strong magnet and then were washed several times with distilled water. The precipitated magnetite was black in color. The powder was then dried in a hot air oven at 50^{o}C overnight. The formation of the amino shell was fabricated by the dispersion of 0.3g of MNSs in 4mL DW, followed by the addition of 600mL of ethanol (99.99%) under sonication for 45min. Subsequently, 10% (v/ v) (3-Aminopropyl) triethoxysilane (APTES) in aqueous solution (80mL) and glycerol (40 mL) were added to the above nanosheets mixture and stirred for 2hr under a nitrogen atmosphere at 90°C. Then, it was let stand for cooling to room temperature, and the nanosheets were washed with DW and methanol. The produced $Fe_3O_4@SiO_2$ nanocomposite was then heated to 50^{o}C up to 7 hours, collected, sorted, and washed three times with ethanol before being dried at 60°C under vacuum oven **(Azzam *et al.*, 2022)**.

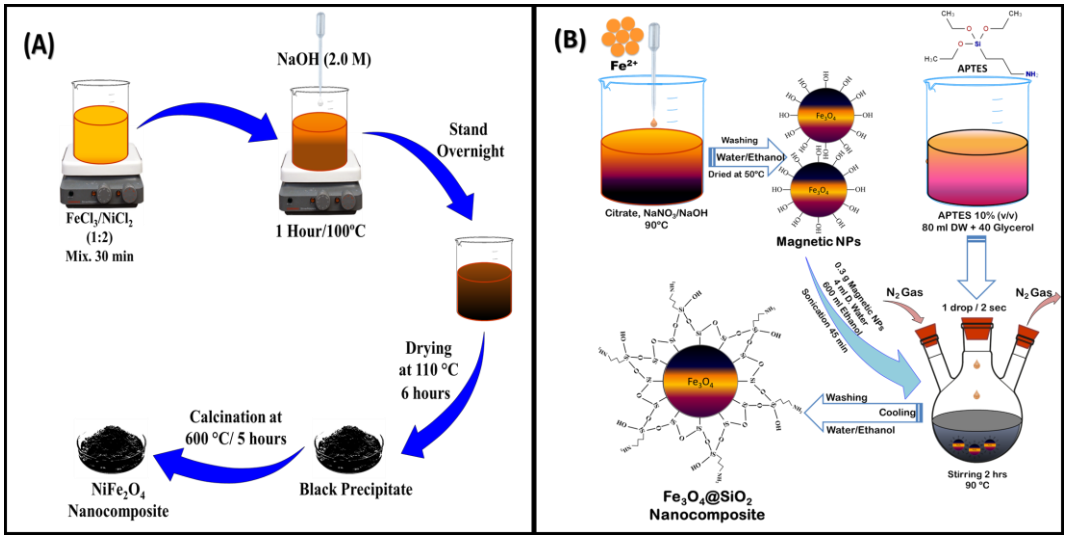

Scheme 1. Synthesis of **A)** $NiFe_2O_4$ and **B)** $Fe_3O_4@SiO_2$ nanocomposites

Characterization of nanocomposites

The infrared spectra were measured with a Pye-Unicam Sp-3-300 Fourier-transform infrared spectrometer (FTIR) equipped with 8101 PC and KBr technique. X-ray diffraction (XRD) measurements were completed with (Bruker AXS-D8, Germany) and CuKαradiation (λ = 1.5406 Å) in the 2θ range from 10 to 80°C. The transmission electron microscopy images were recorded by a JEOLJEM-1400EX transmission electron microscope (Osaka, Japan). To distribute the powders in the samples for TEM investigations, they were suspended in ethanol, and then a drop of the sample was placed on a lacey carbon copper grid to serve as TEM support. The grid was dried under a reduced pressure for 2 hours at room temperature. The accelerating voltage of the TEM was 20kV.

Treatment of hospital wastewater (HWW) by nanocomposites

Filtrated HWW was used to determine the degradation capacity of two nanocomposites for different chemical contaminants. Firstly, 0.1gm of each nanocomposite ($Fe_3O_4@SiO_2$ and $NiFe_2O_4$) was added to 1.0L of HWW and put on a magnetic stirrer for one hour at room temperature. Secondly, treated HWW samples were filtrated and stored at -20°C for further chemical analysis before and after treated with both nanocomposites for detection removal capacities.

Chemical analysis for HWW

Sample preparation and injection

Acetonitrile (200µl) was mixed with 10µl of the filtered untreated HWW and nano-treated samples as a spike. Following an instantaneous 30-second vortex of the solutions, 800µl of 0.1% formic acid in acetonitrile were added to each sample, followed by a 15-minute sonication and a 15-minute centrifugation at 13,000rpm. The supernatant

was then put into the LCMS/ MS analysis's auto sampler vails **(Fabregat-Safont *et al.*, 2023)**.

LCMS /MS instrumentation

Sample analysis was conducted using an Agilent liquid chromatography system (USA), interfaced to a triple quadrupole mass spectrometer Xevo TQ-STM, equipped with an orthogonal Z-Spray electrospray ionization interface (ESI) (Waters Corp, Manchester, UK). The UHPLC separation was performed using an Atlantis T3 analytical column (3.0 × 150mm, 3µm particle size, Waters Corp.) maintained at 40°C. The two mobile phases, (A) water and (B) methanol, were supplied at a flow rate of 0.4mL/ min, together with 2mM ammonium acetate and 0.1% formic acid. The mobile phase gradient was maintained for 10min to allow column re-equilibration. It was as follows: 0min, 10% B; 6min, 99% B; 8min, 99%; 8.10min, 10% B; and. The injection volume was 100µL. ESI was operated in a positive ionization mode (ESI+), using a capillary voltage of 1kV. The flow rates of nitrogen desolvation gas and cone gas were set at 1200L/ h and 250L/ h, respectively. The temperature of the source was fixed at 150°C, and the temperature of the desolvation was set at 650°C **(Fabregat-Safont *et al.*, 2023)**.

HPLC/ UV conditions

Two methods were applied for the detection of the selected drugs, including paracetamol, diclofenac, sulfamethoxazole, ketoprofen, amoxicillin, ofloxacin, and oxytetracycline by HPLC/ UV high-performance liquid chromatography method with UV detection. Chromatographic conditions: An Agilent HPLC/ UV detector and C18 column was used with a mobile phase consisting of a combination of acetonitrile and water (with or without the addition of buffer and/or acid) at a specific ratio. The flow rate was optimized for the separation of the drugs. The first method, effective chromatographic separation was achieved for paracetamol, diclofenac, sulfamethoxazole, and amoxicillin using Waters Symmetry C18 column, (3.9 X 150mm, 5µm particle sizes) with gradient elution of the mobile phase composed of 0.05M orthophosphoric acid and acetonitrile. The gradient elution began with 5% (by volume) acetonitrile, increased linearly to 65% in 5min, and kept constant until the run was finished. A 1.5mL/ min flow rate was managed to pump the mobile phase. The multiple wavelength detector was calibrated at 220nm, and the medicines were quantified by determining their peak regions **(Belal *et al.*, 2015)**. However, the second method, separation of ketoprofen, ofloxacin, and oxytetracycline was achieved with C18, 250 × 4.60mm 5µ column, low-pressure gradient mode with an ambient temperature and mobile phase comprising acetonitrile-water containing 0.1% orthophosphoric (20:80). The stream rate was 1ml/ min, and the fluency was monitored spectrophotometrically at 310nm instead of 316nm in the reference. Quantitation involved determining the amount of each drug by comparing its peak area or height with

that of an ordinary calibration curve prepared from known concentrations of the drugs **(Sirisha *et al.*, 2014)**.

RESULTS AND DISCUSSION

1. Characterization of synthesized nanocomposites

1.1. FTIR spectral measurements

Fig. (1A) represents the FTIR spectrum of the magnetic nickel ($NiFe_2O_4$ NC) nanocomposites, revealing two principal absorption bands in the range of 400– 600cm^{-1}. The first band was around 474cm^{-1}, and the second one was around 584cm^{-1}, credited to the elongated bond length of oxygen metal ions in the octahedral sites and the shorter bond length of oxygen–metal ions in the tetrahedral places in the spinel structure, respectively. Many OH groups were presented on the surface of the NC showing a broad absorption band at about 3421cm^{-1} for the stretching mode of H_2O molecules. However, Fig. (1B) illustrates the FTIR spectra of magnetic silica (Fe_3O_4@SiO_2) NC, where FTIR spectrum of Fe_3O_4 nanoparticles showed bands at 584 and 453cm^{-1} due to the intrinsic stretching vibrations of Fe–O and Ni–O in the spinel structures, respectively (**Kurnaz Yetim *et al.*, 2020)**. For the SiO_2-coated Fe_3O_4 nanoparticles connected to the Fe–O stretching vibration, the band was detected at 563cm^{-1}. The band is a distinctive band that shows the octahedral orientation of Fe–O tension. The band was detected at 558cm^{-1} in the FTIR spectra of a pure Fe_3O_4 nanostructure, and two bands appeared in the region of 1500– 1700cm^{-1} which are assigned to an asymmetric stretching mode of adsorbed carbonate groups. On the other hand, the Fe_3O_4@SiO_2 FTIR spectrum showed a slight change, which was recognized to the TEOS covering. Moreover, peaks were observed at 1090, 965, and 801cm^{-1}, which represent Si–O–Si stretching vibration peaks, that further support the presence of TEOS coating. Wide band observed at 3000– 3500cm^{-1} (attributed to the C–H stretching bond) illustrates silanol (Si–OH) and H–OH related stretching vibrations **(Qu *et al*., 2014)**.

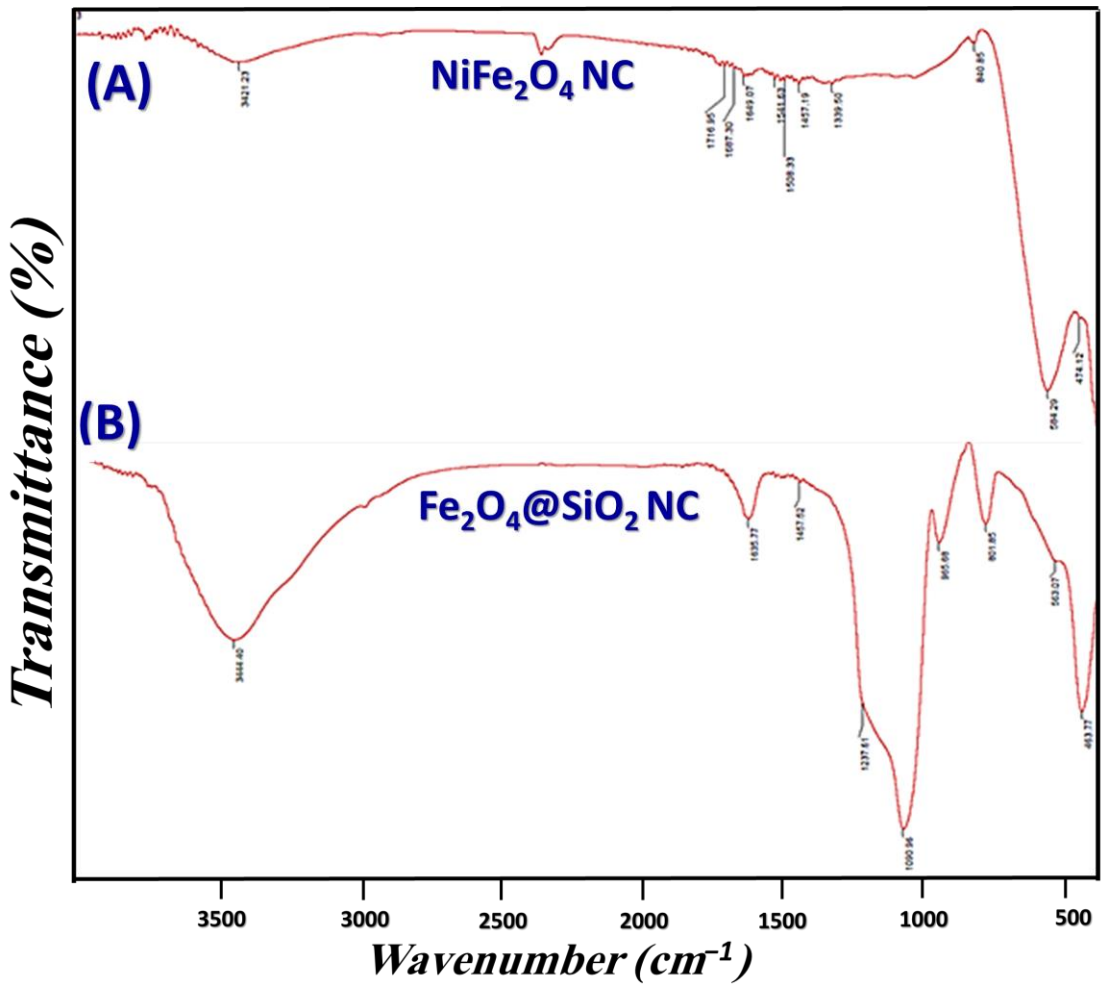

Fig. 1. FTIR spectra of **A)** $NiFe_2O_4$ and **B)** $Fe_3O_4@SiO_2$ nanocomposites

1.2. X-ray diffraction (XRD) patterns of analysis

The samples' crystalline nature is indicated by the pointed and sharp peaks of the XRP's pattern. This is very much essential for the photocatalytic activity in such a way that high crystallinity reduces the amount of trapping electrons and, thus, decreases the possibility of recombination. The XRD patterns (Fig. 2A) indicate the structure of cubic spinal crystal structure of $NiFe_2O_4$ NC according to the standard of JCPDS (Card no. 10-0325) **(Qu *et al.*, 2007)**, with no diffraction peaks of other impurities, as for instance Fe_2O_3 or NiO peaks. In the case of $NiFe_2O_4$ nanoparticles, there are seven sharp diffraction peaks with 2θ values at 30.24, 35.48, 36.94, 43.06, 53.80, 57.20, and 62.88° relating to the crystal planes of 220, 311, 222, 400, 422, 511, and 440, respectively. One explanation for this is the manifestation of amorphous SiO_2. This confirmed that the modification method did not alter the modified nanoparticles' crystalline structure, suggesting that the surface alteration and conjugation of the Fe_3O_4 nanoparticles had no effect on the magnetite particles' physical characteristics. The mean crystallite size for Fe_3O_4 NPs was established to be 7.6nm, which is basically in accordance with the TEM

result **(Hassan *et al.*, 2020)**.

The XRD patterns of the prepared Fe_3O_4@SiO_2 nanoparticles are displayed in Fig. (2B). The generated Fe3O4's diffraction pattern revealed noticeably distinct peaks at 35.4, 30.1, and 62.5°, corresponding to the 311, 220, and 440 planes of the inverse spinel crystal structure. This diversion pattern for Fe_3O_4 nanoparticles was identical to that of the JCPDS card (JCPDS No. 19-0629) **(Husain *et al.*, 2019)**. Regarding Fe_3O_4@SiO_2, noise was noted beneath the 40° region, and each peak's breadth grew, particularly at smaller angles. This happened due to a modest expansion in the interplanar distance and tension on the Fe_3O_4 nanoparticle surface between the Fe3O4 core and the SiO_2 shell **(Nikmah *et al.*, 2019)**. This outcome also happened in the dual Fe_3O_4@SiO_2 and porous Fe_3O_4@SiO_2. In these circumstances, the noise in the 40° region was stronger than the dense Fe_3O_4@SiO_2 noise. This noise suggests that there may be an amorphous phase present at the surface. The SiO_2 covering layer on the surface of the Fe_3O_4 nanoparticles is formed by an amorphous phase with Si–O–Si bonding, as indicated by the FTIR spectra **(Cha *et al.*, 2020)**.

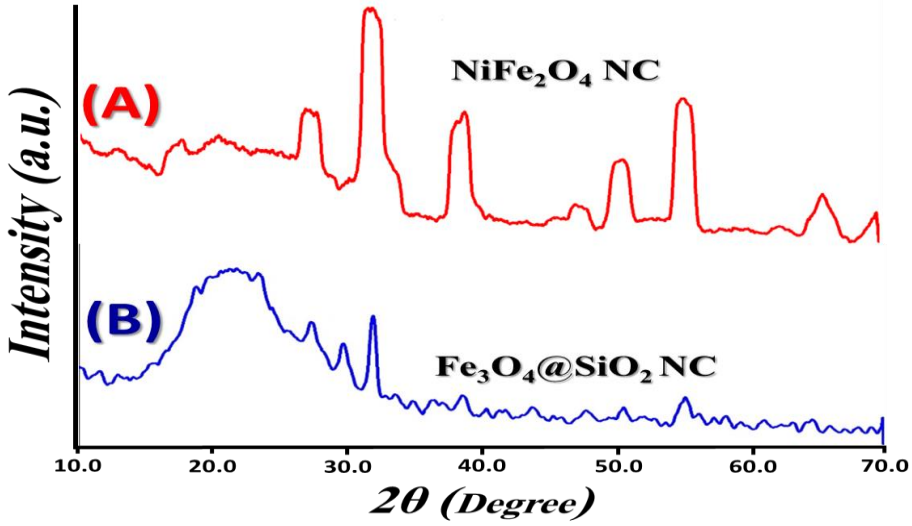

Fig. 2. X-ray diffraction (XRD) patterns of A) $NiFe_2O_4$ and B) Fe_3O_4@SiO_2 nanocomposites

1.3. SEM-TEM images and EDX spectrum

The morphological features were studied to $NiFe_2O_4$ and Fe_3O_4@SiO_2 NCs using SEM and TEM, while EDX analysis was also performed to confirm the chemical structure of the nanocomposites.

As shown in Fig. (3), the TEM image of $NiFe_2O_4$ NC showed that the nanoparticles have a uniform, cubic structural morphology with distribution agglomeration. The average size was between 13.8 & 16.7nm. However, previous study showed that $NiFe_2O_4$ presents a characteristic surface with an agglomeration of small

particles that leads to a porous structure with a rough surface **(Shao *et al.*, 2012)**. **Alamier *et al*. (2023)** detected the TEM image of the $NiFe_2O_4$ NC, which are spherical in shape. The $NiFe_2O_4$ NPs, particle numbers of distributions lie in the narrow size domains ranging from 2 to 6nm. Fig. (4) displays the SEM images of $Fe_3O_4SiO_2$ NC that revealed the formation of spherical particles. TEM images clearly illustrate the core@shell structure of the $Fe_3O_4@SiO_2$ NC. The TEM images confirm that Fe_3O_4 nanoparticles were perfectly coated with SiO_2 where the core@shell $Fe_3O_4@SiO_2$ NC structure was successfully obtained. The TEM images of $Fe_3O_4@SiO_2$ NC revealed that the average size of nanocomposite was about 17.8nm, and they were found to be in the agglomerated form. For the porous and dual $Fe_3O_4SiO_2$NC, they were similar in size at 66.8nm for the porous and ~52.1– 60.0nm for the dual. **Han *et al*. (2021)** assessed that the thickest SiO_2 layer of the dense $Fe_3O_4SiO_2$NC was 24.7nm. Moreover, the dual layer comprised the SiO_2 shell of the dual $Fe_3O_4SiO_2$ NC, with thicknesses of around 15.6–27.9nm for the dense layer and 24.2– 44.4nm for the porous layer. For the porous and dual $Fe_3O_4@SiO_2$ NC, almost spherical forms were seen, while the dense $Fe_3O_4@SiO_2$ NC showed a significantly rougher structure. Moreover, **Xu *et al.* (2013)** showed that the size of the MNPs slightly increased to 8nm after the modification of Fe_3O_4 using TEOS. An amino layer was further coated on the surface of the constructed $Fe_3O_4@SiO_2$ NC, producing $Fe_3O_4@SiO_2$-NH_2 NC, with an average size of 10nm.

The chemical composition of two nanocomposites was performed by EDX analysis, as shown in Fig. (5). The EDX results of $NiFe_2O_4$ NC are exhibited in Fig. (1B). Clear O, Fe, and Ni peaks were detected with WT percentages of 26.96, 58.52, and 14.52, respectively. While EDX results of $Fe_3O_4@SiO_2$ NC are stated in Fig. (3B). Clear O, Fe and Si peaks were detected with WT percentages of 42.88, 39.52, and 17.60, respectively.

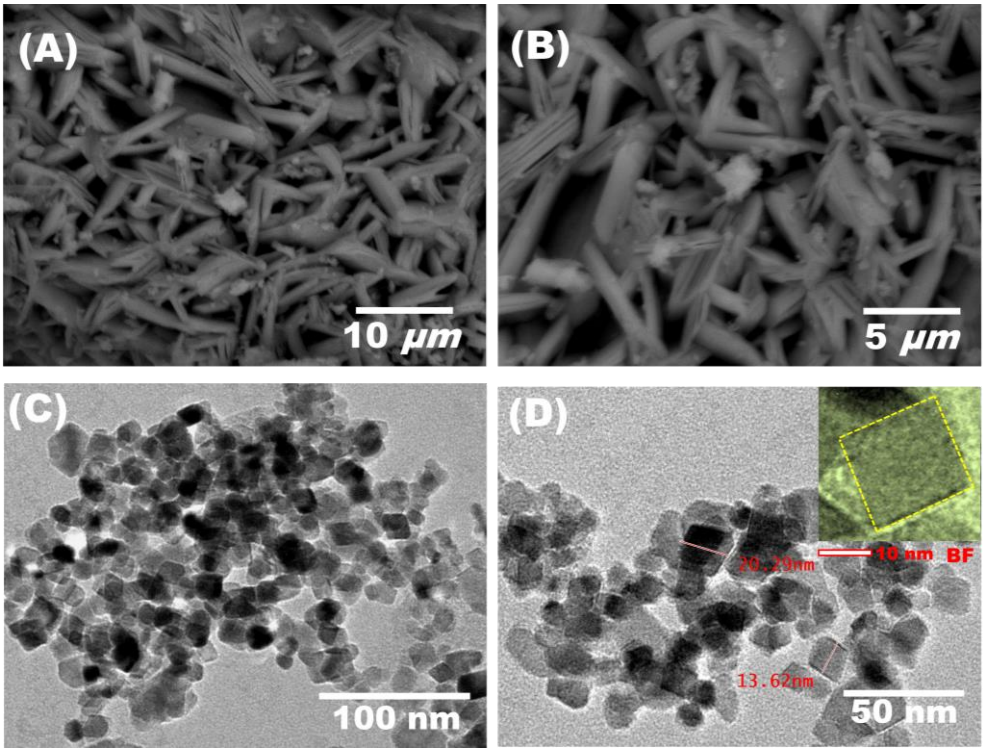

Fig. 3. (A, B) SEM and **(C, D)** TEM images of $NiFe_2O_4$ nanocomposite at different magnifications

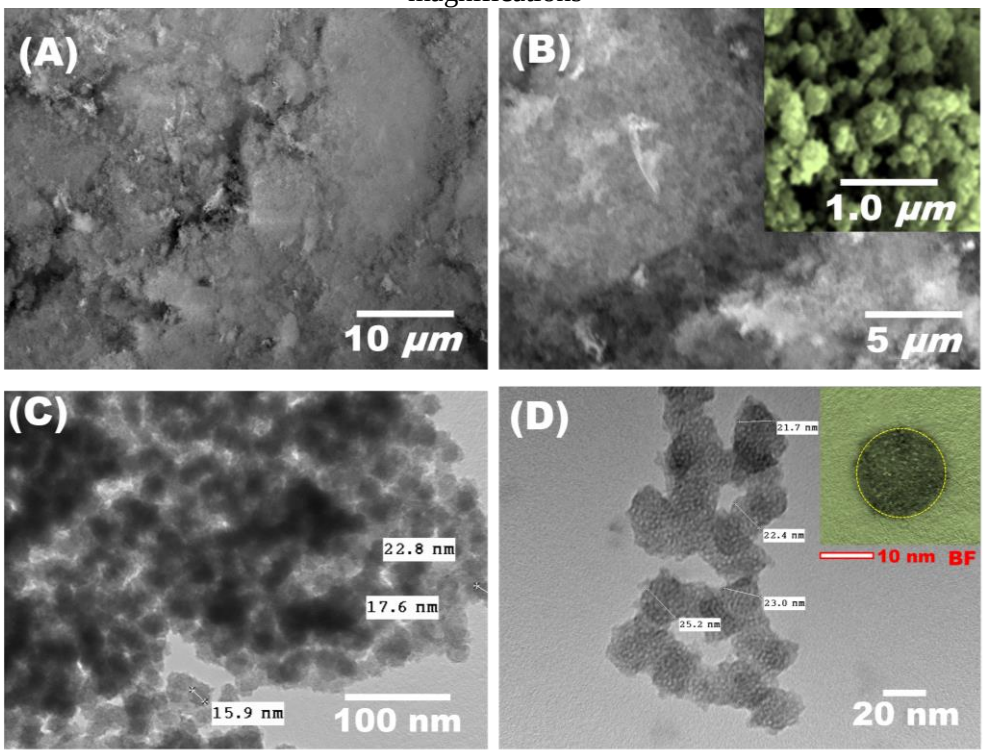

Fig. 4. (A, B) SEM and **(C, D)** TEM images of $Fe_3O_4@SiO_2$ nanocomposite at different magnifications

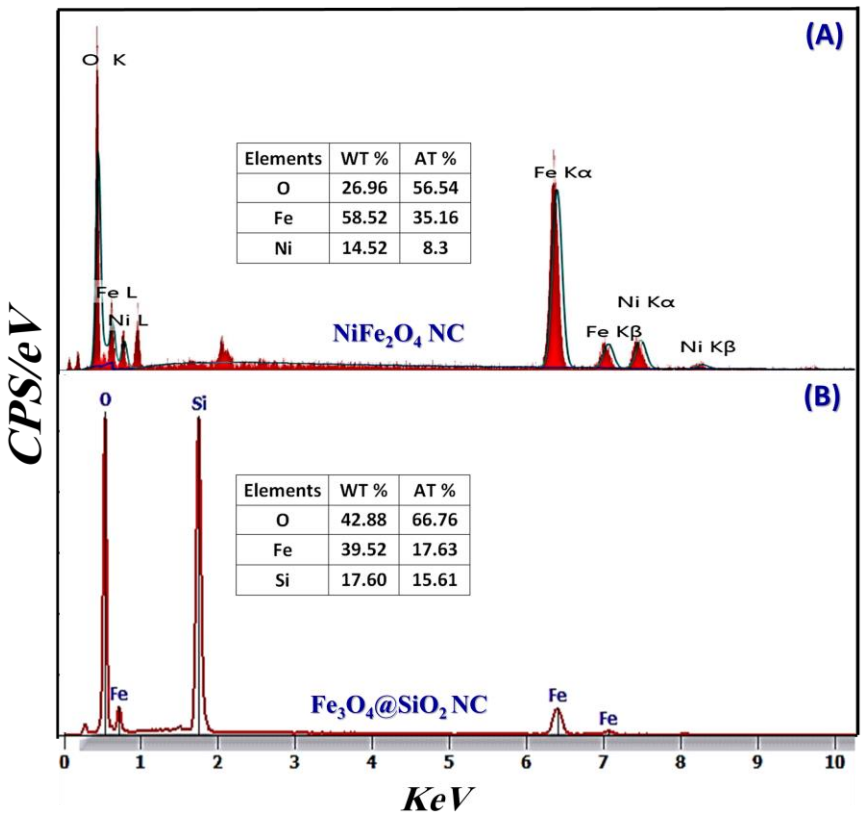

Fig. 5. EDX spectra of **A)** $NiFe_2O_4$ and **B)** $Fe_3O_4@SiO_2$ nanocomposites

2. Chemical analysis of HWW

The screening of the HWW by LCMS/ MS showed that countless compounds were present in the HWW, as shown in Fig. (6) and Table (1). These 49 pharmaceutical compounds were divided into analgesics, antibiotics, anesthetics, decongestants, antidepressants, antipsychotics, beta-blockers, phthalates, chemotherapy, and anticancer drugs. The present data agree with previous results of twelve pharmaceutical compounds which were examined in the study of **Qarni *et al.* (2016)** regading the influents and effluents of two hospital wastewater treatment plants (HWWTPs) in Saudi Arabia. These compounds included atenolol, erythromycin, cyclophosphamide, paracetamol, bezafibrate, carbamazepine, ciprofloxacin, caffeine, clarithromycin, lidocaine, sulfamethoxazole, and nacetylsulfamethoxazol (NACS). Addtionally, **Bírošová *et al.* (2020)** monitored about 38 substances in hospital wastewater with the highest concentrations observation for tramadol, citalopram, venlafaxine, cotinine, atenolol, valsartan, carbamazepine, azithromycin, and ciprofloxacin. In the current work, most of them were found. **Arsand *et al.* (2018)** evaluated samples composition by liquid chromatography coupled to time-of-flight mass spectrometry (LC-qTOF-MS/MS) for observing 300 pharmaceuticals and pesticides in environmental water samples. They devised and qualitatively validated a quick and easy wide-scope screening approach for emerging organic contaminants (ECs) detection in aqueous samples. The samples from

surface water (SW) and effluent wastewater (EW) were used in the validation investigation. 170 substances, including medications and insecticides, were found and verified, even in the worst-case scenario (EW). In contrast to other global regions, most African and Asian nations have relatively few reports about the occurrence of pharmaceuticals in the environment, with numerous reports coming from Africa, namely South Africa **(Ngubane *et al.*, 2019)**. The literature, however, indicates that different medicinal types found are dependent on several similar agricultural, social, technological, and cultural elements found in a variety of geographic locations and bodies of water. In the Nairobian River basin, paracetamol, ibuprofen, zidovudine, and sulfamethoxazole have been found in values ranging from 10– 30µg L^{-1}, according to a study conducted in Kenya by **K'oreje *et al.* (2012)**. Additionally, research conducted in KwaZulu-Natal's Umgeni River, South Africa, revealed the existence of several drug classes in surface water and sediments, including antipyretic, antiepileptic, antibiotic, and antipsychotic, at amounts greater than 10µg L^{-1} **(Ngubane *et al.*, 2019)**. In Asia, there are few studies reporting the incident of pharmaceuticals in the natural environment, yet their consumption rate is increasing **(Menon *et al.*, 2020)**. Monitoring the dissemination and presence of these chemicals in Asian and African water bodies is therefore crucial.

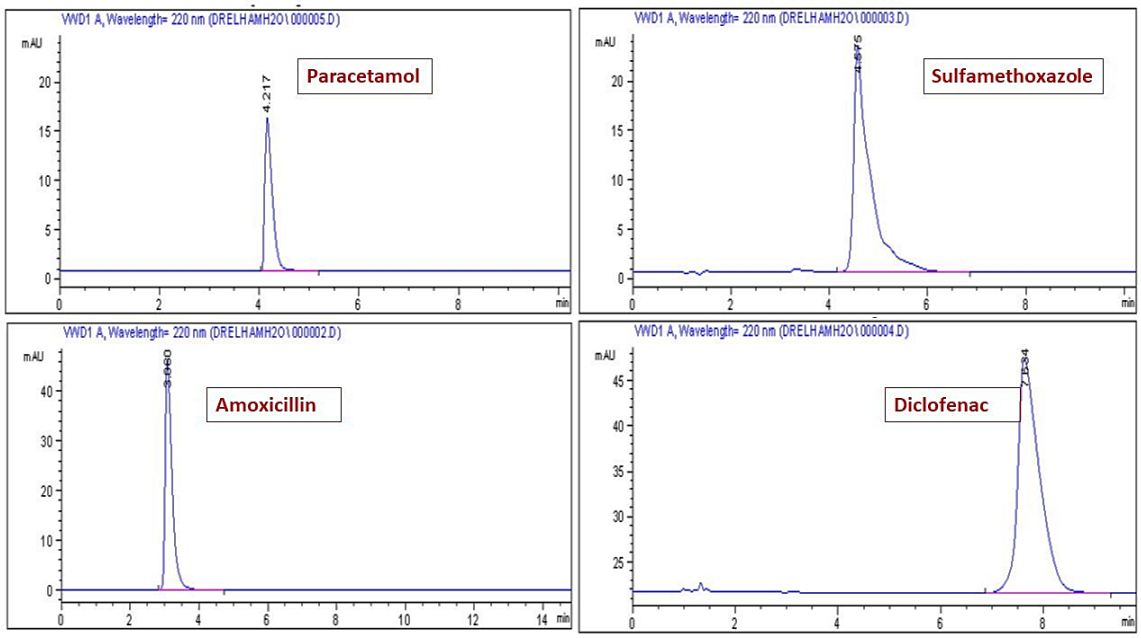

Fig. 6. Different standards used in HPLC/ UV detection of some analgesics and antibiotics at a wavelength of 220nm

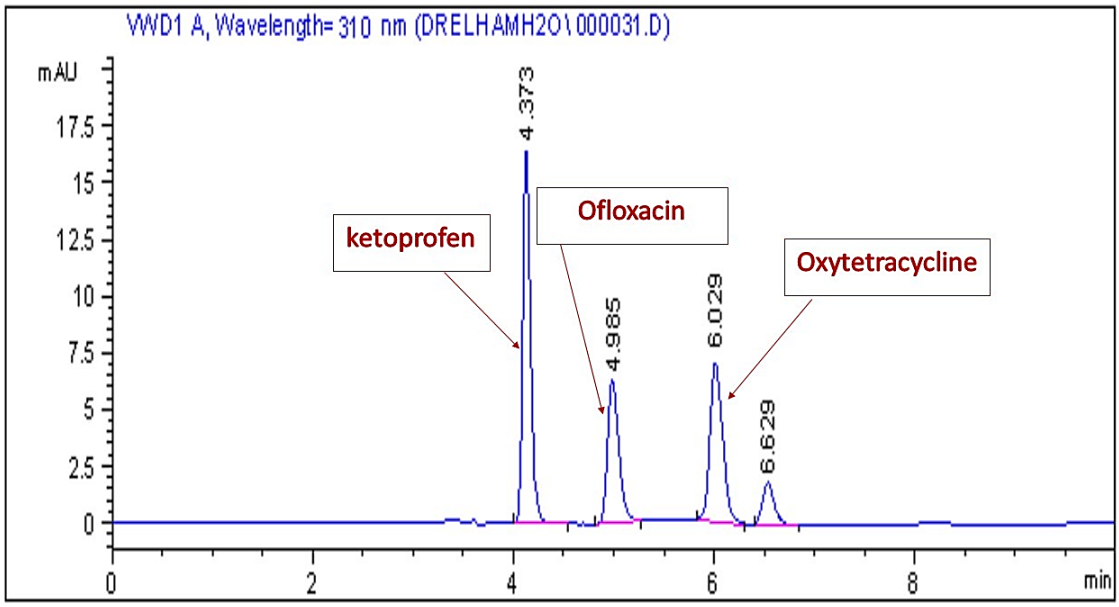

Fig. 7. Different standards used in HPLC/ UV detection of some analgesics and antibiotics at a wavelength of 310nm

3. Removal capacity of nanocomposites

The data presented in Figs (8- 10) and Table (2) show the concentration of seven different analgesics and antibiotics in the HWW and the samples treated with $NiFe_2O_4$ and $Fe_3O_4@SiO_2$ NCs. The diclofenac, sulfamethoxazole, amoxicillin, and oxytetracycline drugs were completely removed after being treated with $NiFe_2O_4$ and $Fe_3O_4@SiO_2$ NCs with RT of 7.16, 7.63, 3.08, 6.03min, respectively. Whereas paracetamol was completely removed by $Fe_3O_4@SiO_2$ NCs at RT of 4.57min. These data coincide with those recorded in a study by **Pylypchuk *et al.* (2018)**, who found that $Fe_3O_4@SiO_2$ NC could remove up to 99% of paracetamol and 95% of diclofenac from a mixture simultaneously. Moreover, **Lin *et al.* (2023)** reported a maximum adsorption capacity of 120mg/ g for paracetamol and 80mg/ g for diclofenac using $Fe_3O_4@SiO_2$ NC. Additionally, **Saucier *et al.* (2017)** achieved a 96.77% removal rate for amoxicillin and paracetamol from the aqueous effluents by using the effective activated carbon $CoFe_2O_4$ NC as an adsorbent. Furthermore, various studies have demonstrated the efficacy of $NiFe_2O_4$ nanoparticles in removing diclofenac from water, which was evidenced in the present data. In their study, **Mohammadi *et al.* (2021)** found that $NiFe_2O_4$ nanoparticles could remove up to 95% of diclofenac from water within 60 minutes. Alternatively, **Khodadadi *et al.* (2019)** observed the degradation of tetracycline (TC) using $FeNi_3@SiO_2$ magnetic nanoparticles by Fenton-like treatment method and found a maximum TC degradation efficiency of 87%. This is traced back to the potential of the Fe_3O_4 core providing a large surface area for the adsorption of drug molecules and generating reactive oxygen species (ROS) that can oxidize the drug molecules, breaking

them down into smaller, non-toxic molecules. The silica shell can encapsulate the drug molecules, preventing them from re-entering the water. Some of the previously published assessments highlighted the serious ecological harm posed by NSAIDs through summarizing their origin, distribution, and end of life, whilst other studies examined advanced oxidation progressions (AOPs), biodegradation technologies and adsorption techniques **(Mlunguza *et al.*, 2019; Petrie & Camacho-Muñoz, 2021; Rastogi *et al.*, 2021)**. However, since 2015, different removal methods have advanced so quickly, making it imperative to report the progress made in detail. Furthermore, all the drugs except paracetamol were completely not identified in the $NiFe_2O_4$ NC, while with $Fe_3O_4@SiO_2$ NC, ketoprofen and ofloxacin were only present after the treatment. These results support the data identified from LCMS/ MS analysis which selected the $NiFe_2O_4$ NCs as the best sample in the three examined samples. These may be ascribed at pH< 6.4, the oxygen containing group in $NiFe_2O_4$ forms a positively charged aqua complex and becomes ionized, forming a negative charge on its surface. This explains the high removal efficiency of both adsorbents at low pH values. The disposition of the positive charges on the side of both adsorbents and the nonionized form analgesics and antibiotics does not initiate electrical repulsion **(Lin *et al.*, 2023)**.

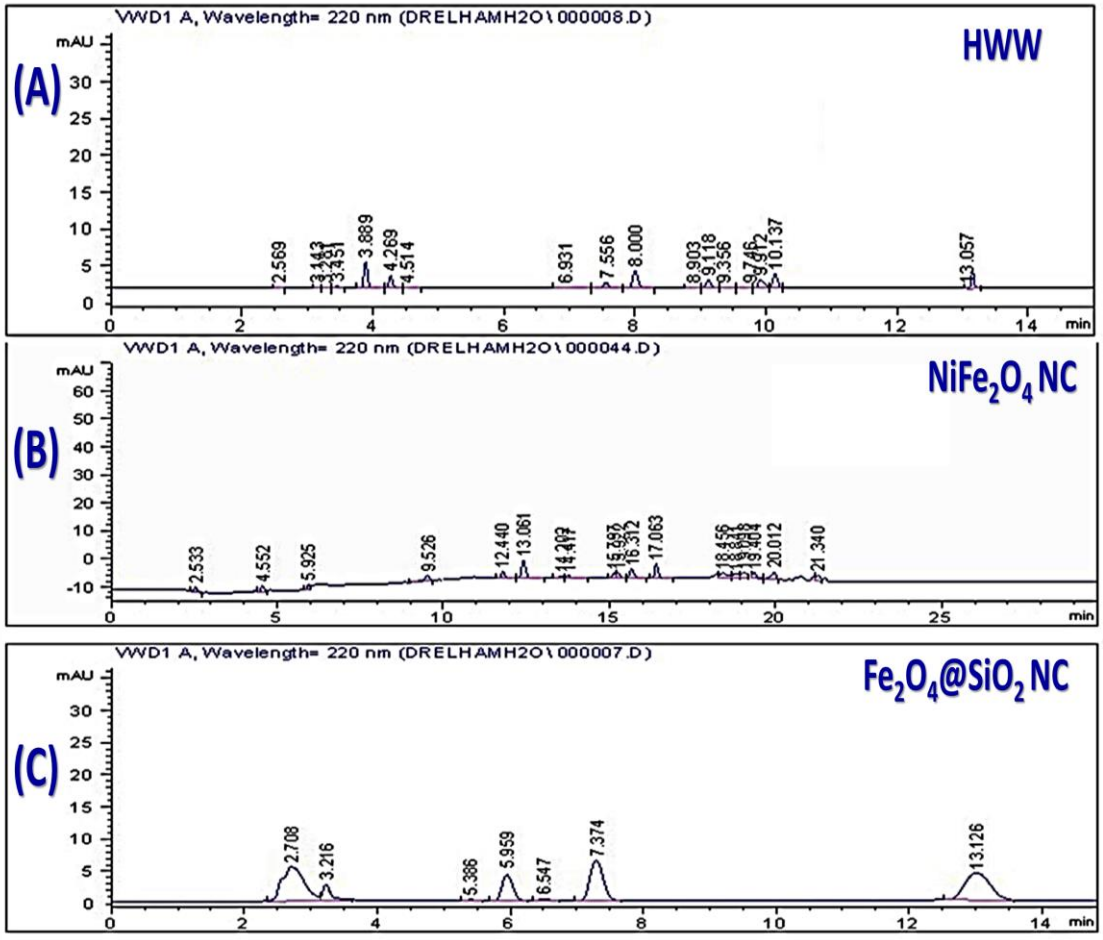

Fig. 8. HPLC/UV at a wavelength of 220nm of the four selected analgesics and

antibiotics (paracetamol, diclofenac, sulfamethoxazole, ketoprofen, and amoxicillin) in **A)** Hospital wastewater (HWW) sample, **B)** HWW treated with $NiFe_2O_4$ NC, and **C)** HWW treated with $Fe_3O_4@SiO_2$ NC

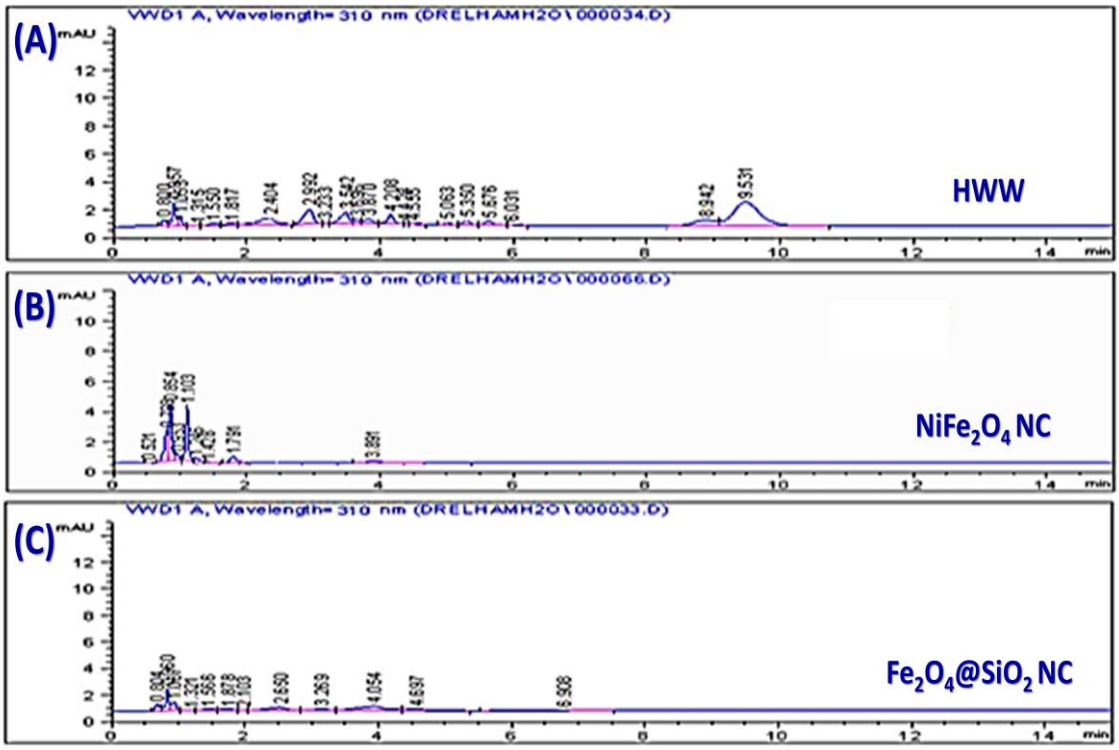

Fig. 9. HPLC/ UV at a wavelength of 310nm of the three selected analgesics and antibiotics (ketoprofen, ofloxacin, and oxytetracycline) in **A)** HWW, **B)** $NiFe_2O_4$ NC, and **C)** $Fe_3O_4@SiO_2$ nanocomposites

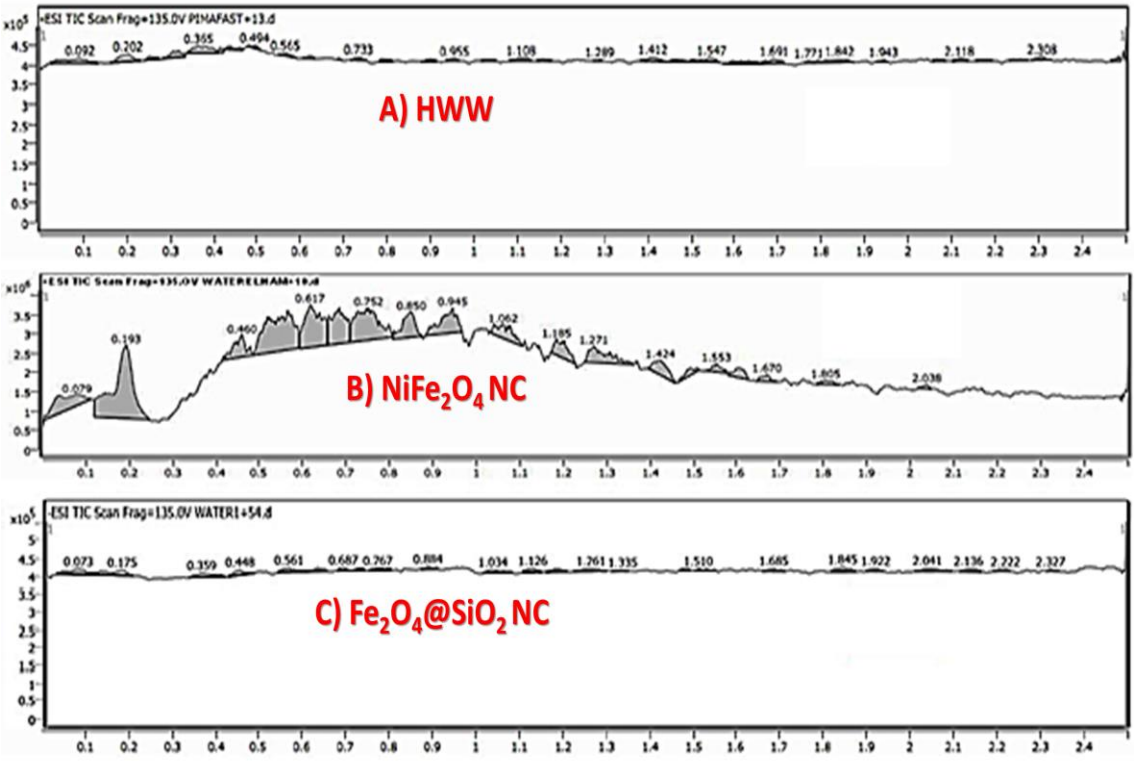

Fig. 10. LCMS/ MS analysis of **A)** Hospital wastewater (HWW) sample, **B)** HWW treated with $NiFe_2O_4$ NC, and **C)** HWW treated with Fe_3O_4@SiO_2 NC

Table 1. Different compounds in hospital wastewater (HWW) and after being treated with two nanocomposites (Samples analyzed by High-Performance Liquid Chromatography Mass Spectrum (LCMS/ MS))

Group	Compound/ Derivative	Formula	MWT	$NiFe_2O_4$ NC	Fe_3O_4@SiO_2 NC
Analgesic	Paracetamol	$C_8H_9NO_2$	151.3	ND	ND
	Ibuprofen	$C_{13}H_{18}O_2$	206.1	ND	+
	Nabumetone	$C_{15}H_{16}O_2$	228.1	ND	+
	Diclofenac	$C_{14}H_{11}C_{l2}NO_2$	296.1	ND	ND
	Cephalexin	$C_{16}H_{17}N_3O_4S$	347.3	ND	ND
	Phenylbutazone	$C_{19}H_{20}N_2O_2$	308.4	ND	ND
	salicylic acid	$C_7H_6O_3$	138.1	ND	+
Anesthetic	Morphine, 2TMS derivative	$C_{23}H_{35}NO_3Si_2$	429.2	ND	++
	Dihydromorphine, 2TMS derivative	$C_{23}H_{37}NO_3Si_2$	431.2	ND	++
	Lidocaine	$C_{14}H_{22}N_2O$	234.1	ND	ND
Decongestant	Naphazoline	$C_{14}H_{14}N_2$	210.1	ND	++
	Pseudoephedrine	$C_{10}H_{15}NO$	165.2	ND	ND
	Norephedrine	$C_9H_{13}NO$	169.2	ND	ND
Antibiotic Fluoroquinolone Sulfonamide	N-acetyl sulfamethoxazole	$C_{12}H_{13}N_3O_4S$	295.3	ND	ND
	Sulfamethoxazole	$C_{10}H_{11}N_3O_3S$	253.6	ND	ND
	Trimethoprim	$C_{14}H_{18}N_4O_3$	290.2	ND	ND
	Oxytetracycline	$C_{22}H_{24}N_2O_9$	460.0	ND	ND
	Chloramphenicol	$C_{11}H_{12}C_{l2}N_2O_5$	323.4	ND	ND
	Ofloxacin	$C_{18}H_{20}FN_3O_4$	361.4	ND	ND
	Penicillin G	$C_{16}H_{18}N_2O_4S$	334.2	ND	+
	Sulfamethazine	$C_{12}H_{14}N_4O_2S$	278.2	ND	ND
	Sulfathiazole	$C_9H_9N_3O_2S_2$	255.4	ND	ND

Antidepressant	**Carbamazepine**	**$C_{15}H_{12}N_2O$**	**236.4**	**ND**	**ND**
	Nordazepam	**$C_{15}H_{11}ClN_2O$**	**270.1**	**ND**	**++**
	Zimeldine	**$C_{16}H_{17}BrN_2$**	**317**	**ND**	**ND**
	Prazepam	**$C_{19}H_{17}ClN_2O$**	**324.1**	**ND**	**+**
	Citalopram	**$C_{20}H_{21}FN_2O$**	**324.3**	**ND**	**ND**
	Desipramine	**$C_{18}H_{22}N_2$**	**266.2**	**ND**	**ND**
Antipsychotic	**Amphetamine**	**C_9H1_3N**	**135.4**	**ND**	**ND**
	Benzphetamine	**$C_{17}H_{21}N$, HCl**	**239.1**	**++**	**+**
	Fluspirilene	**$C_{29}H_{31}F_2N_3O$**	**475.3**	**ND**	**ND**
	Ephedrine	**$C_{10}H_{15}NO$**	**165.2**	**ND**	**ND**
	Caffeine	**$C_8H_{10}N_4O_2$**	**195.1**	**ND**	**ND**
β-Blocker	**Atenolol, Practolol**	**$C_{14}H_{22}N_2O_3$**	**266.2**	**ND**	**ND**
	Metoprolol	**$C_{15}H_{25}NO_3$**	**267.4**	**ND**	**ND**
	Sotalol	**$C_{12}H_{20}N_2O_3S$**	**272.4**	**ND**	**ND**
Phthalate	**Phthalic anhydride**	**$C_8H_4O_3$**	**148**	**ND**	**++**
	Isophthalaldehyde	**C_8H_6O**	**134**	**ND**	**++**
	Tetrafluorophthalic acid	**$C_8H_2F_4O$**	**238**	**ND**	**++**
	Bisphenol C	**$C_{14}H_{10}C_{l2}O_2$**	**256.2**	**ND**	**+**
	Dibutyl phthalate	**$C_{16}H_{22}O_4$**	**278.2**	**ND**	**ND**
Nonsteroidal anti-inflammatory	**p-amino-phenol**	**C_6H_7NO**	**109**	**ND**	**ND**
	5-Hydroxyflunixin	**$C_{14}H_{11}F_3N_2O_3$**	**312.2**	**ND**	**ND**
Chemotherapy and anticancer drugs	**Altretamine**	**$C_9H_{18}N_6$**	**210.2**	**ND**	**++**
	Chloranthalactone A	**$C_{15}H_{16}O_2$**	**228.1**	**ND**	**+**
	Aminoglutethimide	**$C_{13}H_{16}N_2O_2$**	**232.2**	**ND**	**+**
	Pentetic Acid (DTPA)	**$C_{14}H_{23}N_3O_{10}$**	**393.1**	**ND**	**++**

Note: The data in the table were suggested as the MWT comparison according to https://webbook.nist.gov/chemistry/mw-ser/. ND: not detected, +: the MWT identified once, ++: MWT identified more than once.

Table 2. Concentrations of selected analgesics and antibiotics in hospital wastewater (HWW) and after treated with two nanocomposites

Compound	RT (min)	HWW (µg/dL)	$NiFe_2O_4$ NC (µg/dL)	$Fe_3O_4@SiO_2$ NC (µg/dL)
Paracetamol	**4.57**	**0.11**	**0.1**	**ND**
Diclofenac	**7.16**	**0.59**	**ND**	**ND**
Sulfamethoxazole	**7.63**	**1.89**	**ND**	**ND**
Amoxicillin	**3.08**	**0.09**	**ND**	**ND**
Ketoprofen	**4.37**	**27.26**	**ND**	**26.98**
Ofloxacin	**4.98**	**7.61**	**ND**	**7.47**
Oxytetracycline	**6.03**	**0.86**	**ND**	**ND**

The results in Table (2) show that sulfamethoxazole, diclofenac, amoxicillin and oxytetracycline drugs were completely vanished at RT of 7.63, 7.16, 3.08 and 6.03min after being treated from $Fe_3O_4@SiO_2$ and $NiFe_2O_4$ NCs. In recent research articles, $Fe_3O_4@SiO_2$ and $NiFe_2O_4$ nanocomposites were investigated for their potential use in removing sulfamethoxazole from water **(Makofane *et al.*, 2022; Ahmed *et al.*, 2023)**. Nanocomposites have a high adsorption capacity for sulfamethoxazole, with a removal efficiency of around 88% within a short equilibrium time of 40 minutes **(Song *et al.*, 2022)**. The absorption of sulfamethoxazole onto $Fe_3O_4@SiO_2$ nanocomposites is primarily through hydrogen bonding and hydrophobic interactions. Conversely, there is a specific mention of $NiFe_2O_4$ nanocomposites, which demonstrated high degradation of

pollutant sulfamethoxazole and could be magnetically separated. It was efficient in transforming sulfamethoxazole into products that may finally yield simple ions and mineral acids **(Nawaz *et al.*, 2020; Makofane *et al.*, 2022)**. However, **Springer *et al.* (2018)** reported the use of magnetic nickel ferrite nanoparticles, which showed a maximum adsorption of 16.8mg g^{-1} for diclofenac; however, the presence of dissolved salts affected the adsorption efficiency, with a removal efficiency remaining between 30–42% for diclofenac. On the other hand, **Da Cunha *et al.* (2023)** described the utilization of polyaniline-coated magnetic nanoparticles (Fe_3O_4/SiO_2/PAni) to enhance the removal of diclofenac. The respectable results were obtained at a pH of 4, with 25mg of adsorbent material, and after 10 minutes of stirring. The material demonstrated an approximately 90% diclofenac elimination effectiveness from aqueous solutions under these optimized circumstances. Moreover, **Wang *et al.* (2012)** elucidated that the adsorption ability of oxytetracycline antibiotic from water by magnetic carbon nanoparticles with core-shell structure increased within a pH range of 3.5- 7.5, while experiencing a decrease with further increase in pH (pH 7.5- 8.5). Differently, the elimination of oxytetracycline in aqueous solutions by magnetic composites of Fe_3O_4@C takes about 44min to absorb 79%. All these factors and characteristics influence the percentage of adsorbed drugs from water supplies and affect the mechanism with core-shell nanoparticles. Some studies indicate that hydrogen bonding, electrostatic interactions and electron-donor-acceptor interactions were the major forces for core-shell adsorption **(Kakavandi *et al.*, 2016)**. Moreover, **Derakhshani *et al*. (2023)** showed that the $NiFe_2O_4$ magnetic nanocomposite could absorb penicillin G with a high maximum adsorption capacity when the following perfect conditions were met: pH= 9, penicillin G concentration: 30g/ L, nanocomposite dose: 0.3g/ L, contact duration: 20min, and time temperature: 313K. As a result, the magnetic NiFe2O4 nanocomposite, which comprises ampicillin and amoxicillin derivatives, has an important level of effectiveness when it comes to adsorbing penicillin G.

The results in Table (2) display that ketoprofen and ofloxacin drugs were completely disappeared at RT of 4.37 and 4.98min after being treated with $NiFe_2O_4$ NCs. However, Fe_3O_4@SiO_2 nanocomposite was less efficient with the adsorption of ketoprofen and ofloxacin that reported 26.98 and 7.47µg/ dL, respectively. The $NiFe_2O_4$/ activated carbon magnetic composite material was efficient to treat a simulated pharmaceutical effluent for ketoprofen, with a removal percentage of 86.46%. There is a lot of assurance for using NiFe2O4/ activated carbon magnetic composite as an adsorbent to remove new pharmaceutical pollutants from diluted solutions **(Fröhlich *et al.*, 2019)**. However, the ternary $BiVO_4$/ g-C_3N_4/$NiFe_2O_4$ nanocomposite employed by **Zhao *et al.* (2021)** showed the ultimate photocatalytic elimination value constant for ofloxacin, measuring 3.8, 16.3, and 71.2 times that of the corresponding pure $BiVO_4$, pure g-C_3N_4, and pure $NiFe_2O_4$ nanocomposite. The performance of ofloxacin degradation was satisfied at a pH of 5.0, 7.0, and 9.0, demonstrating that this ternary $BiVO_4$/ g-

$C_3N_4/NiFe_2O_4$ photocatalyst had a promising prospect in water treatment, regardless of weak acidic and basic condition. The removal efficiencies of river water were 78.4% within 60min which could effectively remove ofloxacin in various aquatic environments, exhibiting a good prospect in water treatment.

The paracetamol drug totally disappeared at RT of 4.57min after being treated with $Fe_3O_4@SiO_2$ NCs. On the other hand, $NiFe_2O_4$ nanocomposite demonstrated an efficient adsorption of paracetamol, with a reported level of 0.1µg/ dL. **Saucier *et al.* (2017)** presented activated carbon (AC)/ $CoFe_2O_4$ nanocomposites were used as adsorbents for the successful removal of paracetamol (PCT) of aqueous effluents. In a medium comprising nine pharmaceutical materials, including paracetamol, magnetic carbons were successfully employed as adsorbents to treat simulated hospital effluents, eliminating at least 93.00% activated carbon (AC)/ $CoFe_2O_4$ benzoates and 96.77% activated carbon (AC)/ $CoFe_2O_4$ oxalates. **Oliveira *et al.* (2023)** elucidated that after 60 min of reaction, the PCT degradation was 97.5% to cobalt ferrite functionalized in niobium pentoxide. $CoFe_2O_4@Nb_5O_2$ was used as a catalyst to aid in the photocatalytic breakdown of the paracetamol (PCT).

CONCLUSION

Some analgesics and antibiotics which are currently classified as micropollutants, will eventually raise concerns, just like pesticides did. A survey was conducted to detect pharmaceutical compounds prescription to the hospital. Based on the survey, the most prescribed 49 pharmaceutical compounds were divided into analgesics, antibiotics, anesthetics, decongestants, antidepressants, antipsychotics, beta-blockers, phthalates, chemotherapy, and anticancer drugs in hospital wastewater. The synthesized $Fe_3O_4@SiO_2$ and $NiFe_2O_4$ NCs showed an excellent controlled particle production, confirming its ability to completely degrade different analgesics and antibiotics at a pH of 6.5, catalyst dosage of 0.1g/ L, paracetamol, diclofenac, sulfamethoxazole, and an oxytetracycline drugs' concentration of 1µg/ dL, and a time of 60min. The adsorption mechanism is mainly attributed to hydrogen bonding and electrostatic interactions between the nanocomposites and the pharmaceutical compounds. The adsorbent's magnetic characteristic makes post-use separation and recovery simple, effective, and quick. The synthesized $NiFe_2O_4$ NC was efficient to treat a detected pharmaceutical effluent, presenting a removal percentage higher than 85%. Moreover, the material can be easily separated from the liquid phase by a simple magnetic field, thereby significantly reducing separation costs and making it highly efficient for water purification processes. The $NiFe_2O_4$ NC is therefore an innovative material for the absorption of medications from aqueous solutions.

ACKNOWLEDGEMENT

The authors would like to acknowledge Ain Shams University for funding this research through a project entitled "Assessment of hospital wastewater disposal hazards with a special scope on designing biological model and nanocomposite for treatment."

ETHICAL STATEMENT

This study was conducted with the strict recommendations and approval of Research Ethics Committee in the Faculty of Woman for Arts, Ain Shams University, with a Code: sci1332402002.

REFERENCES

Abdallah, A. M. A.; Hammouda, O. and Abdallah, H. M. (2020). Occurrence of antibiotics and antibiotic-resistant bacteria in hospital wastewater in Egypt. Journal of Environmental Management, 253: 109729.

Ahmed, A.; Usman, M.; Ji, Z.; Rafiq, M.; Ullah, R.; Yu, B.; Shen, Y. and Cong, H. (2023). Reduced graphene oxide supported CoFe2O4 composites with enhanced peroxymonosulfate activation for the removal of sulfamethoxazole: Collaboration of radical and non-radical pathways. Journal of Environmental Chemical Engineering, p.110452.

Akhtar, M. S. and Bhanger, M. I. (2010). Removal of heavy metals from wastewater using carbon nanotubes. Separation and Purification Technology, 72(3), 242-251.

Alamier, W. M.; Hasan, N. Nawaz, M. S.; Ismail, K. S.; Shkir, M.; Malik, M. A. and Oteef, M. D. (2023). Biosynthesis of NiFe2O4 nanoparticles using Murayya koenigii for photocatalytic dye degradation and antibacterial application. Journal of Materials Research and Technology, 22: 1331-1348.

Arsand JB.; Hoff RB. and Jank L. (2018). Wide-Scope Determination of Pharmaceuticals and Pesticides in Water Samples: Qualitative and Confirmatory Screening Method Using LC-qTOF-MS. Water Air Soil Pollut (2018) 229: 399.

Azzam A.M.; Shenashen M.A.; Selim M.S.; Mostafa B.; Tawfik, A. and El-Safty S.A. (2022). Vancomycin-loaded furriness amino magnetic nanospheres for rapid detection of gram-positive water bacterial contamination. *Nanomaterials*, *12*(3): 510.

Bao X.; Qiang Z.; Chang J.H.; Ben W. and Qu J. (2014) Synthesis of carbon-coated magnetic nano composite (Fe_3O_4@C) and its application for sulfonamide antibiotics removal from water. Journal of Environmental Sciences 26: 962-969.

Belal T.S.; Bedair M.M.; Gazy A.A. and Guirguis K.M. (2015). Validated Selective HPLC–DAD Method for the Simultaneous Determination of Diclofenac Sodium and Lidocaine Hydrochloride in Presence of Four of Their Related Substances and Potential Impurities. *Acta Chromatographica 27(3): 477–493.*

Bírošová L.; Lépesová K.; Grabic R. and Mackuľak T. (2020). Non-antimicrobial pharmaceuticals can affect the development of antibiotic resistance in hospital wastewater. Environmental Science and Pollution Research 27:13501–13511

Cha, J. H.; Choi, H. H.; Jung, Y. G.; Choi, S. C. and An, G. S. (2020). Novel synthesis of core–shell structured Fe3O4@ SiO2 nanoparticles via sodium silicate. *Ceramics International*, *46*(10): 14384-14390.

Chen, X., Di, L., Yang, H., & Xian, T. (2019). A magnetically recoverable CaTiO3/reduced graphene oxide/NiFe2O4 nanocomposite for dye degradation under simulated sunlight irradiation. *Journal of the Ceramic Society of Japan*, *127*(4), 221-231.

Da Cunha, R.; Silva, C.F.; dos Santos, A.C.; Teixeira, L.S.; Dinali, L.A.F.; do Carmo Batista, W.V.F.; Nascimento Jr, C.S. and Borges, K.B. (2023). Polyaniline-coated magnetic nanoparticles to enhance removal of diclofenac from aqueous media. Surfaces and Interfaces, 43: 103534.

Derakhshani, E., Naghizadeh, A. and Mortazavi-Derazkola, S. (2023). Phyto-assisted synthesis of magnetic NiFe2O4 nanocomposite using the Pulicaria gnaphalodes methanolic extract for the efficient removal of an antibiotic from the aqueous solution: a study of equilibrium, kinetics, isotherms, and thermodynamics. AQUA—Water Infrastructure, Ecosystems and Society, 72(11): 2035-2051.

Eslami, A.; Amini, M.M.; Yazdanbakhsh, A.R.; Rastkari, N.; Mohseni-Bandpei, A.; Nasseri, S.; Piroti, E.; Asadi, A. (2015). Occurrence of non-steroidal anti-inflammatory drugs in Tehran source water, municipal and hospital wastewaters, and their ecotoxicological risk assessment. Environ. Monit. Assess. 187, 734.

Fabregat-Safont D.; Gracia-Marín E.; Ib´anez M.; Pitarch E. and Hern´andez F. (2023). Analytical key issues and challenges in the LC-MS/MS determination of antibiotics in wastewater. Analytica Chimica Acta, 1239: 340739.

Fathy, M.A.; Kamel, A.H. and Hassan, S.S. (2022). Novel magnetic nickel ferrite nanoparticles modified with poly (aniline-co-o-toluidine) for the removal of hazardous 2, 4-dichlorophenol pollutant from aqueous solutions. *RSC advances*, *12*(12): 7433-7445.

Fröhlich, A. C.; Foletto, E. L. and Dotto, G. L. (2019). Preparation and characterization of NiFe2O4/activated carbon composite as potential magnetic adsorbent for removal of ibuprofen and ketoprofen pharmaceuticals from aqueous solutions. Journal of Cleaner Production, 229: 828-837.

Hamad, M.T.M.H. and El-Sesy, M.E. (2023). Adsorptive removal of levofloxacin and antibiotic resistance genes from hospital wastewater by nano-zero-valent iron and nano-copper using kinetic studies and response surface methodology. *Bioresources and Bioprocessing*, *10*(1): 1.

Han, J. S. and An, G. S. (2021). Preparation of dual-layered core–shell Fe3O4@ SiO2 nanoparticles and their properties of plasmid DNA purification. *Nanomaterials*, *11*(12): 3422.

Hassan, S. S.; Kamel, A. H.; Hassan, A. A.; Amr, A. E. G. E.; El-Naby, H. A. and Elsayed, E. A. (2020). A sno2/ceo2 nano-composite catalyst for alizarin dye removal from aqueous solutions. *Nanomaterials*, *10*(2): 254.

Husain, S. A. D. A. N. G.; Irfansyah, M.; Haryanti, N. H.; Suryajaya, S.; Arjo, S., and Maddu, A. (2019). Synthesis and characterization of Fe3O4 magnetic nanoparticles from iron ore. In *Journal of Physics: Conference Series* 1242(1): 01202.

Kakavandi B; Takdastan A; Jaafarzadeh N; Azizi M; Mirzaei A and Azari, A. (2016) Application of Fe_3O_4@C catalyzing heterogeneous UV-Fenton system for tetracycline removal with a focus on optimization by response surface method. Journal of Photochemistry and Photobiology A: Chemistry 314: 178-188.

Kesari, K.K.; Soni, R.; Jamal, Q.M.S.; Tripathi, P.; Lal, J.A.; Jha, N.K.; Siddiqui, M.H.; Kumar, P.; Tripathi, V. and Ruokolainen, J. (2021). Wastewater treatment and reuse: a review of its applications and health implications. *Water, Air, & Soil Pollution*, *232*: 1-28.

Khan, S. A.; Alam, M. Z. and Malik, A. (2019). Hospital wastewater management: A review. Journal of Environmental Management, 236; 753-766.

Khodadadi, M.; Panahi, A.H.; Al-Musawi, T.J.; Ehrampoush, M.H. and Mahvi, A.H., (2019). The catalytic activity of FeNi3@ SiO2 magnetic nanoparticles for the degradation of tetracycline in the heterogeneous Fenton-like treatment method. *Journal of Water Process Engineering*, *32*: 100943.

K'oreje, K. O.; Demeestere, K.; De Wispelaere, P.; Vergeynst, L.; Dewulf, J. and Van Langenhove, H. (2012). From multi-residue screening to target analysis of pharmaceuticals in water: development of a new approach based on magnetic sector mass spectrometry and application in the Nairobi River basin, Kenya. *Science of the Total Environment*, *437*: 153-164.

Kosma C.I.; Lambropoulou D.A. and Albanis T.A. (2010) Occurrence and removal of PPCPs in municipal and hospital wastewaters in Greece. J Hazard Mater 179(1-3): 804–817.

Kosma, C.I.; Kapsi, M.G.; Konstas, P.S.G.; Trantopoulos, E.P.; Boti, V.I.; Konstantinou, I.K. and Albanis, T.A., (2020). Assessment of multiclass pharmaceutical active compounds (PhACs) in hospital WWTP influent and effluent samples by UHPLC-Orbitrap MS: Temporal variation, removals and environmental risk assessment. *Environmental research*, *191*: 110152.

Kumar, S.; Yadav, S.; Kataria, N.; Chauhan, A.K.; Joshi, S.; Gupta, R.; Kumar, P.; Chong, J.W.R.; Khoo, K.S. and Show, P.L. (2023). Recent Advancement in Nanotechnology for the Treatment of Pharmaceutical Wastewater: Sources, Toxicity, and Remediation Technology. Current Pollution Reports, 1-33.

Kurnaz Yetim, N.; Kurşun Baysak, F.; Koç, M. M. and Nartop, D. (2020). Characterization of magnetic Fe 3 O 4@ SiO 2 nanoparticles with fluorescent properties for potential multipurpose imaging and theranostic applications. *Journal of Materials Science: Materials in Electronics*, *31*: 18278-18288.

Li, H.; Li, Y.; Li, Y.; Li, X. and Li, G. (2019). Silver nanoparticles for the removal of pathogens from wastewater. Environmental Science and Pollution Research, 26(6): 5626-5637.

Lin, J. Y.; Zhang, Y.; Bian, Y.; Zhang, Y. X.; Du, R. Z.; Li, M.; Tan, Y. and Feng, X. S. (2023). Non-steroidal anti-inflammatory drugs (NSAIDs) in the environment: Recent updates on the occurrence, fate, hazards and removal technologies. *Science of The Total Environment*, 166897.

Makofane, A.; Maake, P. J.; Mathipa, M. M.; Matinise, N.; Cummings, F. R.; Motaung, D. E. and Hintsho-Mbita, N. C. (2022). Green synthesis of NiFe2O4 nanoparticles for the degradation of Methylene Blue, sulfisoxazole and bacterial strains. Inorganic Chemistry Communications, 139: 109348.

Menon, N. G.; Mohapatra, S.; Padhye, L. P.; Tatiparti, S. S. V. and Mukherji, S. (2020). Review on occurrence and toxicity of pharmaceutical contamination in Southeast Asia. *Emerging Issues in the Water Environment during Anthropocene: A South East Asian Perspective*, 63-91.

Mlunguza, N. Y.; Ncube, S.; Mahlambi, P. N.; Chimuka, L. and Madikizela, L. M. (2019). Adsorbents and removal strategies of non-steroidal anti-inflammatory drugs from contaminated water bodies. *Journal of Environmental Chemical Engineering*, *7*(3): 103142.

Mohammadi, Z.; Kelishami, A. R. and Ashrafi, A. (2021). Application of Ni0. 5Zn0. 5Fe2O4 magnetic nanoparticles for diclofenac adsorption: isotherm, kinetic and thermodynamic investigation. *Water Science and Technology*, *83*(6): 1265-1277.

Nawaz, M.; Shahzad, A.; Tahir, K.; Kim, J.; Moztahida, M.; Jang, J.; Alam, M.B.; Lee, S.H.; Jung, H.Y. and Lee, D.S. (2020). Photo-Fenton reaction for the degradation of sulfamethoxazole using a multi-walled carbon nanotube-NiFe2O4 composite. Chemical Engineering Journal, 382: 123053.

Ngubane, N. P.; Naicker, D.; Ncube, S.; Chimuka, L. and Madikizela, L. M. (2019). Determination of naproxen, diclofenac and ibuprofen in Umgeni estuary and seawater: A case of northern Durban in KwaZulu–Natal Province of South Africa. *Regional Studies in Marine Science*, *29*: 100675.

Nikmah, A.; Taufiq, A. and Hidayat, A. (2019). Synthesis and characterization of Fe3O4/SiO2 nanocomposites. In *IOP Conference Series: Earth and Environmental Science* 276(1): 012046).

Nurdan, K. Y.; Fatma, K. B.; Koç, M. M. and Dilek, N. (2020). Characterization of magnetic Fe 3 O 4@ SiO 2 nanoparticles with fluorescent properties for

potential multipurpose imaging and theranostic applications. *Journal of Materials Science. Materials in Electronics*, *31*(20): 18278-18288.

Oliveira, J.R.; Ribas, L.S.; Napoli, J.S.; Abreu, E.; Diaz de Tuesta, J.L.; Gomes, H.T.; Tusset, A.M. and Lenzi, G.G. (2023). Green magnetic nanoparticles CoFe2O4@ Nb5O2 applied in paracetamol removal. Magnetochemistry, 9(8): 200.

Patrolecco, L.; Ademollo, N.; Grenni, P.; Tolomei, A.; Caracciolo, A. B. and Capri, S. (2013). Simultaneous determination of human pharmaceuticals in water samples by solid phase extraction and HPLC with UV-fluorescence detection. *Microchemical Journal*, *107*: 165-171.

Petrie, B. and Camacho-Muñoz, D. (2021). Analysis, fate and toxicity of chiral non-steroidal anti-inflammatory drugs in wastewaters and the environment: a review. *Environmental chemistry letters*, *19*(1): 43-75.

Pylypchuk, I. V.; Kessler, V. G. and Seisenbaeva, G. A. (2018). Simultaneous removal of acetaminophen, diclofenac, and Cd (II) by Trametes versicolor laccase immobilized on Fe3O4/SiO2-DTPA hybrid nanocomposites. *ACS Sustainable Chemistry & Engineering*, *6*(8): 9979-9989.

Qarni H.A.I.; Collier P.; O'Keeffe J. and Akunna J. (2016). Investigating the removal of some pharmaceutical compounds in hospital wastewater treatment plants operating in Saudi Arabia. Environ Sci Pollut Res (2016) 23:13003–13014.

Qu, F.; Wang, Y.; Liu, J.; Wen, S.; Chen, Y. and Ruan, S. (2014). Fe3O4–NiO core–shell composites: hydrothermal synthesis and toluene sensing properties. *Materials Letters*, *132*, 167-170.

Qu, S.; Wang, J.; Kong, J.; Yang, P. and Chen, G. (2007). Magnetic loading of carbon nanotube/nano-Fe3O4 composite for electrochemical sensing. *Talanta*, *71*(3): 1096-1102.

Rastogi, A.; Tiwari, M.K. and Ghangrekar, M.M. (2021). A review on environmental occurrence, toxicity and microbial degradation of Non-Steroidal Anti-Inflammatory Drugs (NSAIDs). *Journal of Environmental Management*, *300*: 113694.

Saguti, F.; Magnil, E.; Enache, L.; Churqui, M. P.; Johansson, A.; Lumley, D.; Davidsson, F.; Dotevall, L.; Mattsson, A.; Trybala, E. and Lagging, M. (2021). Surveillance of wastewater revealed peaks of SARS-CoV-2 preceding those of hospitalized patients with COVID-19. *Water Res.* 189: 116620.

Sanusi, I.O.; Olutona, G.O.; Wawata, I.G. and Onohuean, H. (2023). Occurrence, environmental impact and fate of pharmaceuticals in groundwater and surface water: a critical review. *Environmental Science and Pollution Research*, *30*(39): 90595-90614.

Saucier, C.; Karthickeyan, P.; Ranjithkumar, V.; Lima, E.C.; Dos Reis, G.S. and de Brum, I.A. (2017). Efficient removal of amoxicillin and paracetamol from

aqueous solutions using magnetic activated carbon. Environmental Science and Pollution Research, 24: 5918-5932.

Shao, L.; Ren, Z.; Zhang, G.; Chen, L. (2012). Facile synthesis, characterization of a MnFe 2O 4/activated carbon magnetic composite and its effectiveness in tetracycline removal. Mater. Chem. Phys. 135: 16-24.

Sim, W.J.; Lee, J.W.; Lee, E.S.; Shin, S.K.; Hwang, S.R. and Oh, J.E. (2011). Occurrence and distribution of pharmaceuticals in wastewater from households, livestock farms, hospitals and pharmaceutical manufactures. Chemosphere 82: 179–186.

Sirisha T.; Gurupadayya BM. and Sridhar S. (2014). Simultaneous Determination of Ciprofloxacin and Tinidazole in Tablet Dosage Form by Reverse Phase High Performance Liquid Chromatography. Tropical Journal of Pharmaceutical Research (6): 981-987.

Song, Y.; Jiang, T.; Wu, J.; Chen, J. and Du, Q. (2022). Effect of dissolved silicate on the degradation of sulfamethoxazole by nZVI@ D201 nanocomposite. Journal of Molecular Liquids, 368: 120767.

Springer, V.; Barreiros, L.; Avena, M. and Segundo, M. A. (2018). Nickel ferrite nanoparticles for removal of polar pharmaceuticals from water samples with multi-purpose features. Adsorption, 24: 431-441.

Wang, .X.; Zhang, D.; Niu, H.Y.; Meng, Z.F. and Cai, Y.Q. (2012). Synthesis of Core/ Shell Structured Magnetic Carbon Nanoparticles and Its Adsorption Ability to Chlortetracycline in Aquatic Environment. College of Science 33: 1234-1240.

Wu, F.; Li, X.; Zhang, L.; Li, Y. and Gao, H. (2019). Graphene oxide for adsorption and removal of pharmaceuticals and personal care products from wastewater. Chemosphere, 221: 272-281. doi: 10.1016/j.chemosphere.2018.12.068.

Xu, J.; Ju, C.; Sheng, J.; Wang, F.; Zhang, Q.; Sun, G. and Sun, M. (2013). Synthesis and characterization of magnetic nanoparticles and its application in lipase immobilization. *Bulletin of the Korean Chemical Society*, *34*(8): 2408-2412.

Yuan, T. and Pia, Y. (2023). Hospital wastewater as hotspots for pathogenic microorganisms spread into aquatic environment: a review. *Front. Environ. Sci*. 10:1734. doi: 10.3389/fenvs.2022.1091734.

Zhang, H.; Lv, L.; Zhao, Y. and Wu, J. (2018). Nanomaterials in wastewater treatment: An overview of applications, limitations and future perspectives. Journal of Environmental Sciences, 71: 92-110. doi: 10.1016/j.jes.2018.02.002.

Zhang, Y.; Chen, J.; Yang, S. and Xie, Y. (2017). The application of nanotechnology in wastewater treatment: A review. Journal of Nanoscience and Nanotechnology, 17(8): 5175-5190.

Zhao, G.; Ding, J.; Zhou, F.; Chen, X.; Wei, L.; Gao, Q.; Wang, K. and Zhao, Q. (2021). Construction of a visible-light-driven magnetic dual Z-scheme BiVO4/g-C3N4/NiFe2O4 photocatalyst for effective removal of ofloxacin: mechanisms and degradation pathway. Chemical Engineering Journal, 405: 126704.

Zorita, S.; Mårtensson, L. and Mathiasson, L. (2009). Occurrence and removal of pharmaceuticals in a municipal sewage treatment system in the south of Sweden. Sci. Total Environ. 407: 2760–2770.